

## The Rac1 Exchange Factor Dock5 Is Essential for Bone Resorption by Osteoclasts

Virginie Vives<sup>1,2,\*</sup>, Mélanie Laurin<sup>3</sup>, Gaele Cres<sup>1,2</sup>, Pauline Larrousse<sup>1,2</sup>, Zakia Morichaud<sup>4</sup>, Danièle Noel<sup>5</sup>, Jean-François Côté<sup>3</sup>, and Anne Blangy<sup>1,2</sup>

<sup>1</sup>Montpellier Universities 1 and 2, CRBM, Montpellier, France

<sup>2</sup>CNRS, UMR5237, Montpellier, France

<sup>3</sup>Institut de Recherches Cliniques de Montréal, Université de Montréal, Montreal, Quebec H2W 1R7, Canada

<sup>4</sup>CNRS, UMR5236, CPBS, Montpellier, France

<sup>5</sup>INSERM U844, Montpellier, France

### Abstract

Osteoporosis, which results from excessive bone resorption by osteoclasts, is the major cause of morbidity for elder people. Identification of clinically relevant regulators is needed to develop novel therapeutic strategies. Rho GTPases have essential functions in osteoclasts by regulating actin dynamics. This is of particular importance because actin cytoskeleton is essential to generate the sealing zone, an osteoclast-specific structure ultimately mediating bone resorption. Here we report that the atypical Rac1 exchange factor Dock5 is necessary for osteoclast function both in vitro and in vivo. We discovered that establishment of the sealing zone and consequently osteoclast resorbing activity in vitro require Dock5. Mechanistically, our results suggest that osteoclasts lacking Dock5 have impaired adhesion that can be explained by perturbed Rac1 and p130Cas activities. Consistent with these functional assays, we identified a novel small-molecule inhibitor of Dock5 capable of hindering osteoclast resorbing activity. To investigate the in vivo relevance of these findings, we studied *Dock5*<sup>-/-</sup> mice and found that they have increased trabecular bone mass with normal osteoclast numbers, confirming that Dock5 is essential for bone resorption but not for osteoclast differentiation. Taken together, our findings characterize Dock5 as a regulator of osteoclast function and as a potential novel target to develop antiosteoporotic treatments.

### Keywords

OSTEOCLAST; RAC1; DOCK5; ADHESION; INHIBITOR OF BONE RESORPTION

---

Address correspondence to: Anne Blangy, PhD, Rho GTPase Signaling Pathways, CNRS, UMR5237, CRBM, 1919 route de Mende, Montpellier, France. anne.blangy@crbm.cnrs.fr.

\*Present address: IGMM, CNRS UMR5535, Montpellier, France.

### Disclosures

All the authors state that they have no conflicts of interest.

Additional Supporting Information may be found in the online version of this article.

## Introduction

Osteoporosis is now a major health problem worldwide, in particular owing to general population aging. An important cause of osteoporosis is estrogen deficiency that results in excessive bone loss in postmenopausal women. Diverse conditions such as bone metastases, lack of physical activity, disability, and inflammation also provoke osteoporosis. Although the mechanisms of these diseases are distinct, excessive activity of osteoclasts (OCs) is a common feature and hallmark of osteoporosis.<sup>(1)</sup> OCs, the major bone-resorbing cells, are derived from mononuclear precursors of the monocyte/macrophage lineage, such as bone marrow macrophages (BMMs). In response to the cytokines, receptor activator of NF- $\kappa$ B ligand (RANKL), and macrophage colony-stimulating factor (M-CSF), monocyte precursors differentiate into pre-OCs that ultimately fuse to form polykaryons with the capacity to resorb mineralized substrates such as bone.<sup>(2)</sup> To initiate bone resorption, OCs polarize and undergo extensive morphologic changes to form an actin ring, also known as the *sealing zone*.<sup>(3)</sup> This OC-specific adhesion structure is composed of densely packed podosomes.<sup>(4)</sup> It surrounds the ruffled border, a differentiated region of the plasma membrane that secretes protons and proteases at bone contact. This is the actual site of bone resorption.<sup>(5)</sup> The activation of RANK receptor by RANKL elicits a complex transcriptional program during OC differentiation. The master OC transcription factor, NFATc1, regulates many OC-specific genes, in particular *ATP6v0d2* and *DC-STAMP* (involved in precursor fusion) and *Acp5*, *Ctsk*, *Src*, and *ITGB3*, essential for bone resorption.<sup>(6)</sup> At the bone surface, OCs cycle between resorptive and migratory phases. Assembly and disassembly of the sealing zone require profound remodeling of the actin cytoskeleton,<sup>(7)</sup> regulated by adhesion signaling molecules, including Src, Pyk2, and p130Cas, downstream of integrin  $\alpha$ v $\beta$ 3.<sup>(8)</sup> As major cellular regulators of actin organization, Rho GTPase signaling pathways are also essential players in sealing zone assembly.<sup>(9)</sup>

Rho GTPases cycle between inactive GDP-bound and active GTP-bound states. In their active form, they bind to effector proteins and engage numerous signaling pathways. Efficient nucleotide replacement requires guanine nucleotide exchange factors (GEFs) that catalyze activation of Rho GTPases.<sup>(10)</sup> These GEFs fall into two families: Dbl and Dock proteins. The Dock family of GEFs consists of 11 Dock1-related proteins (also known as *Dock180-related proteins*) in mammals.<sup>(11,12)</sup> Docks are characterized by a unique DHR-2 (or CZH-2) domain that catalyzes nucleotide exchange on Rac1 or Cdc42 and a DHR-1 domain that localizes the GEFs to phosphatidylinositol(3,4,5)phosphate-enriched membranes. Dock1, Dock2, and Dock5 also contain an SH3 domain at the N terminus and a polyproline domain at the C terminus. Through these domains, Dock1 interacts with CrkII, Crk-L, and ELMO proteins and promotes Rac1 activation for efficient actin remodeling, cell migration and adhesion, and myoblast and macrophage fusion.<sup>(12–15)</sup>

In a previous study we found that RANKL activates the transcription of *Dock5*.<sup>(16)</sup> In addition, Dock5 is among the membrane-associated proteins most significantly overexpressed in OCs as compared with macrophages.<sup>(17)</sup> Here we tested the idea that Dock5 could be a central player in the control of OC cytoskeleton dynamics and biologic activity. We demonstrate that Dock5 is essential for formation of the sealing zone and consequently for bone resorption by OCs. In addition, interfering with Dock5 expression

abrogated Rac1 activation and impaired OC integrin-mediated adhesion. Likewise, blocking Dock5-mediated activation of Rac1 using a novel small biochemical inhibitor strikingly decreased OC resorption activity. Importantly, mice bearing a genetic deletion of *Dock5* have increased trabecular bone mass, in agreement with a role of this GEF in bone resorption. Our findings therefore identify a novel molecular mechanism that regulates actin dynamics for sealing zone assembly in OCs. They further highlight Dock5 as a potential target for novel antiosteoporotic treatments.

## Materials and Methods

### Mice

*Dock5*<sup>-/-</sup> mice were described previously.<sup>(14)</sup> Mice used were 4 to 8 weeks old and were maintained at the animal facilities of the CNRS in Montpellier, France, and of the IRCM in Montreal, Quebec, Canada.

### Histologic analyses

Femurs of 8-week-old mice were fixed for 1 week in 10% formalin in PBS and embedded in Histo-resin (Leica, Nanterre, France), and 7- $\mu$ m sections were stained with von Kossa and counterstained with von Gieson. Alternately, bones were decalcified in 10% EDTA for 10 days and embedded in paraffin, and 4.5- $\mu$ m sections were stained for tartrate-resistant acid phosphatase (TRACP) activity and counterstained with a nuclear fast red. Measures were done in a standard zone in the distal femur situated 250  $\mu$ m from the growth plate excluding the primary spongiosa. Bone volume, total volume, OC numbers, and bone perimeters were measured in the same region of interest on three adjacent slides using Bioquant OSTEO II (Bioquant Image Analysis, Nashville, TN, USA).

### Production of OCs and osteoblasts

BMMs were isolated from long bones of 4- to 8-week-old animals as described previously,<sup>(16)</sup> and OCs were obtained by culturing BMMs with RANKL (100 ng/mL) and M-CSF (10 ng/mL) (Peprotech, Neuilly sur Seine, France) for 5 days. RAW264.7 cells were grown for 5 days with RANKL (50 ng/mL) to obtain OCs. For resorption, OCs were differentiated in multiwell chambers or on coverslips coated with calcium phosphate (Osteologic Biocoat; BD Biosciences, Le Pont de Claix, France) or in 96-well plates containing a bovine bone slice (IDS Nordic Bioscience, Paris, France). Mesenchymal stem cells (MSCs) were isolated from mouse bone marrow and grown as described previously.<sup>(18)</sup> Osteogenesis was induced by culture at low density ( $3 \times 10^4$  cells in 6-well plates) for 21 days in osteogenic medium (DMEM supplemented with 10% fetal bovine serum, 2 mM glutamine, and 0.05 mM ascorbic acid) supplemented with 3 mM NaH<sub>2</sub>PO<sub>4</sub> for mineralization assays. Osteoblasts were characterized by alizarin red S staining of the secreted calcified extracellular matrix, as described previously.<sup>(18)</sup>

### Microscopy, immunofluorescence, and TRACP labeling

OCs were fixed and stained for DNA, actin, or vinculin or TRAP as described previously.<sup>(16,19)</sup> Anti-vinculin antibody (Sigma, St Louis, MO, USA) was revealed with Alexa Fluor 546-conjugated secondary antibody and actin stained with Alexa Fluor 360- or 488-

conjugated phalloidin (Invitrogen, Carlsbad, CA, USA). Preparations were mounted in Mowiol 40–88 (Sigma) and imaged with a Zeiss Axioimager Z2 microscope with Coolsnap HQ2 camera for fluorescence and Coolsnap color Cf camera using a Zeiss 40× PLAN-NEOFLUAR 1.3 oil DIC or Zeiss 20 × PLAN-APOCHROMAT 0.8 or Zeiss 10 × EC PLAN-NEOFLUAR 0.3 (Zeiss, Inc., Thornwood, NY, USA). Images were acquired with MetaMorph 7.0 software (Molecular Devices, Sunnyvale, CA, USA). OC circularity was measured using ImageJ ([rsbweb.nih.gov/ij/index.html](http://rsbweb.nih.gov/ij/index.html), NIH, USA). OCs were counted manually in 96-well plates stained to reveal DNA and TRACP activity, except in Fig. 5F, where they were counted automatically using a Cellomics Arrayscan VTI (Thermo Scientific, Saint Herblain, France). For scanning electron microscopy, OCs on bone slices were fixed in PBS containing 3% glutaraldehyde and postfixed with 1% OsO<sub>4</sub>. After alcohol dehydration, OCs were dried in hexamethyldisilazane (Acros Organics, Geel, Belgium) for 2 minutes, coated with gold-palladium, and observed using a Hitachi (Tokyo, Japan) S4000 scanning microscope at 10 kV.

### Adhesion assays

OCs differentiated in 96-well plates were incubated for 5 minutes in PBS supplemented or not with 0.25 mM EDTA. Wells then were rinsed with PBS, fixed, stained with 0.1% crystal violet, and lysed, and OD595 was measured as described previously.<sup>(19)</sup> Each condition was performed in triplicate wells.

### Plasmid DNAs

Yeast expression vectors for *Rac1* and *kinectin*<sup>(20,21)</sup> and GFP-fused TrioN<sup>(22)</sup> were reported previously. The obtain full-length *Dock5* cDNA, BamHI-KpnI fragment of RIKEN clone E130320D18 (nucleotides 249 to 1913 of *Dock5* mRNA) was fused to the KpnI-NotI fragment of IMAGE clone 30106676 (nucleotides 1914 to 6461 of *Dock5* mRNA). The whole was fused to GFP and was inserted into pMXs-puro,<sup>(23)</sup> a gift from Dr Kitamura (Tokyo, Japan). *Dock5* DHR2 domain (amino acids E1119 to L1667) was cloned into pEGFP (Clontech, Mountain View, CA, USA) or myc tagged in pRs426Met.<sup>(21)</sup> *Dock5* and firefly *luciferase* shRNA expression vectors were described previously,<sup>(16)</sup> as well as methods to produce and use retroviruses.<sup>(16,19)</sup>

### RT-PCR and primers

Reverse-transcriptase polymerase chain reaction (RT-PCR) analyses were performed as described previously.<sup>(19)</sup> Amplification primers were 5′-GGC TGT GTT TAC CGA CGA GC-3′ and 5′-CAA GCA CGC GGA CAA TGT TG-3′ for *calcitonin receptor*, 5′-TCA GCT TCA GCA TTC AGC CC-3′ and 5′-ACT GCA CGA TTC CAG AGT CC-3′ for *Dock1* and 5′-AGC CTT GCA TCT CCT GTG GC-3′ and 5′-CAT GCG TCC CTT GGA TGC TG-3′ for *Dock2*, 5′-GCG CTC TGT CTC TCT GAC CT-3′ and 5′-GCC GGA GTC TGT TCA CTA CC-3′ for *osteocalcin*, 5′-AAT GCC CTG AAA CTC CAA AA-3′ and 5′-AGG GGA ATT TGT CCA TCT CC-3′ for *alkaline phosphatase*, and 5′-TGT TCA GCT TTG TGG ACC TC-3′ and 5′-TCA AGC ATA CCT CGG GTT TC-3′ for *collagen 1*. Other primers were described: *Gapdh*, *Dock5*, *Vav3*, *Src*, *TRACP*, *NFATc1*, *CtsK*, *integrin β3*, *DC-STAMP*, *ATP6v0d2*,<sup>(16,19)</sup> *OSCAR*, *CD44*,<sup>(6)</sup> and *ADAM8*.<sup>(24)</sup>

### Active Rac1 quantification

GTP-bound Rac1 was pulled down from OC or 293T cell extracts using GST-fused PAK1 CRIB domain as described previously<sup>(22)</sup> and revealed by Western blot with monoclonal anti-Rac1 antibodies (Transduction Laboratories, Le Pont de Claix, France) and anti-GFP polyclonal antibodies (Torrey Pines Biolabs, Houston, TX, USA). To activate Rac1, OCs at day 4 of differentiation were starved overnight in the presence of 2% serum, stimulated with 100 ng/mL of M-CSF, or lifted and replated onto vitronectin-coated plates for 30 minutes prior to lysis, and active Rac1 levels were measured using the G-LISA kit according to manufacturer's instructions (Cytoskeleton, Denver, CO, USA).

### Immunoprecipitation, Western blot, and antibodies

Antibodies for phosphorylated Erk-1/2 were from Cell Signaling (Boston, MA, USA) and for total Erk1/2 from Santa Cruz Biotechnology (Santa Cruz, CA, USA). Antibodies for Crk, p130Cas, and Pyk2 were from Transduction Laboratories. 4G10 phosphotyrosine-specific antibodies were a gift from Dr Bettache (Montpellier, France). OCs were lysed in lysis buffer (50 mM Tris, pH 7.5, 120 mM NaCl, 1 mM EDTA, 6 mM EGTA, 1% NP-40, 20 mM NaF, and 100  $\mu$ M Na<sub>3</sub>VO<sub>4</sub>) and analyzed directly by Western blot for total tyrosine phosphorylation analysis. For immunoprecipitation, precleared lysates were precipitated and analyzed by Western blot with the appropriate antibodies. Immune complexes were visualized by the ECL Western Lightning Plus detection system (Perkin Elmer, Villebon sur Yvette, France) with horseradish peroxidase-conjugated secondary antibodies (GE Healthcare, Piscataway, NJ, USA) and quantified using ImageJ.

### Resorption assays

OCs in multiwell Osteologic Biocoat (BD Biosciences) were fixed on day 7 of stained with von Kossa as described previously.<sup>(19)</sup> The entire well surface was imaged using a Zeiss AxioimagerZ1 microscope. The well image was reconstituted, and resorbed areas were measured using MetaMorph 7.0 software (Molecular Devices). For bone-resorption assays, OCs were derived from BMMs in 96-well plates containing bovine bone slices. On day 5 of differentiation, the medium was changed with fresh medium. After 2 days, cross-linked C-telopeptide (CTX) concentrations were measured using Crosslap (IDS Nordic Bioscience). To reveal resorption pits, bone slices were incubated for 1 hour in peroxidase-conjugated wheat-germ agglutinin (WGA) lectin (Sigma) in PBS (20  $\mu$ g/mL), followed by detection of peroxidase activity using SIGMAFAST according to manufacturer's instructions (Sigma).

**Yeast methods**—Screening for Dock5 inhibitors was performed in TAT7 yeast disrupted for *erg6* essentially as described for the RhoGEF TrioN.<sup>(20,21)</sup> Briefly, yeasts were grown in 96-well plates in histidine-free and histidine-complemented dropout medium supplemented with 1% DMSO and 100  $\mu$ M of one of the 2640 chemical compounds to be tested (ChemBridge, San Diego, CA, USA).<sup>(25)</sup> Growth curves were established by measuring OD600. Inhibitors were selected for their ability to inhibit selectively growth acceleration in histidine-free medium conferred by Dock5-DHR2 expression without affecting growth in histidine-supplemented medium.

## Statistical analysis

Statistical significances were determined using the Mann-Whitney nonparametric test.

## Results

### Dock5 is a Rac1 GEF associated with OC adhesion structures

We previously identified *Dock5* as a RhoGEF gene strongly induced during RANKL-stimulated osteoclastogenesis in RAW264.7 cells and BMMs<sup>(16)</sup> (Fig. 1A). Purified antibodies directed against the C-terminal end of Dock5<sup>(14)</sup> confirmed the great increase in Dock5 expression during osteoclastic differentiation of BMMs (Fig. 1B) and RAW264.7 cells (Fig. 1C). Previous in vitro observations suggested that Dock5 could activate the GTPase Rac1.<sup>(26)</sup> To confirm this on endogenous Rac1, we expressed in HEK-293T cells the DHR2 domain of mouse *Dock5*, lying between amino acids M1132 and Y1661 and corresponding to the equivalent domain defined in *Dock1*<sup>(11,27)</sup> (Fig. 1D). Pull-down assays using the GTPase-binding domain of the kinase PAK1 that selectively binds to active Rac1 and Cdc42 showed that Dock5 can activate endogenous Rac1 without affecting Cdc42 activity (Fig. 1E, left panel). Expression of GFP fusion proteins was assessed by Western blot (Fig. 1E, right panel). GFP-tagged full-length Dock5 expressed in RAW264.7 cell-derived OCs colocalizes with vinculin at the podosome belt (Fig. 1F).

### Dock5 is essential for OC function in vitro

To investigate the role of Dock5 in OC biology, we down-regulated *Dock5* in RAW264.7 cells using shRNAs.<sup>(16)</sup> Whereas complete silencing of *Dock5* leads to massive detachment of cells around day 3 of differentiation,<sup>(16)</sup> lower retroviral concentrations leading to moderate silencing of Dock5 protein (Supplemental Fig. S1A) allows efficient formation of TRACP<sup>+</sup> multinucleated cells in response to RANKL (Supplemental Fig. S1B). Strikingly, these OCs seeded on calcium phosphate-coated substrates do not form sealing zones (Supplemental Fig. S1C). Accordingly, they do not resorb the mineral substrate (Supplemental Fig. S1D). Consistently, OCs derived from shDock5-expressing BMMs exhibit very few and small sealing zones (Supplemental Fig. S1E) and have reduced bone-resorbing activity (Supplemental Fig. S1F). This suggests that Dock5 is involved in formation of the sealing zone and then in bone resorption by OCs.

To further study the physiologic role of Dock5 in OCs, we differentiated OCs from primary BMMs isolated from *Dock5*<sup>+/+</sup> and *Dock5*<sup>-/-</sup> mice.<sup>(14)</sup> *Dock5*<sup>-/-</sup> BMMs differentiate into OCs defined as TRACP<sup>+</sup> multinucleated cells (Fig. 2A). But *Dock5*<sup>-/-</sup> OCs fail to assemble sealing zones when seeded on calcium phosphate substrates (Fig. 2B, C), and they do not resorb the calcium phosphate mineral substrate (not shown). Electron micrographs of bone slices seeded with *Dock5*<sup>-/-</sup> OCs showed that they can adhere on bone, but they were never found associated with a resorption pit (Fig. 2D). Staining with WGA lectin showed that bone slices seeded with *Dock5*<sup>-/-</sup> OCs have very few and small resorption pits (Fig. 2E). Measurement of degradation products of C-terminal telopeptide of type 1 collagen (CTX) production in the culture medium indeed confirmed that *Dock5*<sup>-/-</sup> OCs are defective for bone resorption (Fig. 2F). These results characterize Dock5 as being essential for the formation of OC sealing zone and subsequent bone resorption.

## Dock5 is necessary for Rac1 and p130Cas activation in OCs

We next evaluated the importance of Dock5 for RANKL-induced expression of osteoclastic marker genes exploiting *Dock5*<sup>+/+</sup> and *Dock5*<sup>-/-</sup> BMMs. Real-time qualitative PCR did not reveal any defect in the expression of the 12 genes tested (Fig. 3A). In particular, *ITGB3*, *Src*, and *Vav3*, which are involved in sealing zone formation, are expressed at normal levels. We also noticed that Dock5 deficiency does not induce a compensatory overexpression of *Dock1* or *Dock2*, the closest *Dock5* paralogues (Fig. 3B). Thus suppression of Dock5 does not appear to prevent the establishment of the OC-specific transcriptional program.

We then investigated how the absence of Dock5 may affect the activation of Rac1 in OCs. M-CSF regulates OC cytoskeleton<sup>(28)</sup> and induces rapid activation of Rac1, leading to the phosphorylation of Erk1/2.<sup>(29,30)</sup> Integrin  $\alpha\beta3$  stimulation by adhesion of OCs onto vitronectin also activates Rac1.<sup>(29,31)</sup> In the absence of Dock5, we found that M-CSF induces normal Rac1 activation and Erk1/2 phosphorylation (Fig. 3C, D), and adhesion-stimulated activation of Rac1 is not affected (Fig. 3E).

We then looked at the steady-state level of Rac1 activity in adherent OCs under no stimulation. In this case, active Rac1 pulldown assays showed a strong reduction in Rac1 activity in OCs derived from *Dock5*<sup>-/-</sup> BMMs or from RAW264.7 cells expressing *Dock5* shRNAs (Fig. 4A, B). *Dock5*<sup>-/-</sup> OCs exhibited very irregular shapes on plastic (Fig. 4C), as confirmed by significantly reduced circularity (Fig. 4D). Furthermore, *Dock5*<sup>-/-</sup> OCs are less resistant to detachment from the substrate on EDTA treatment (Fig. 4E). These results show that in the absence of Dock5, OCs have low levels of Rac1 activity associated with spreading and adhesion defects.

We next investigated candidate signaling molecules known to participate in the control of OC adhesion that could be linked to Dock5 and Rac1 signaling. The adaptor protein p130Cas is involved in actin organization in OCs.<sup>(32-34)</sup> Dock1 is known to stimulate signaling from the CrkII-p130Cas complex by increasing p130Cas tyrosine phosphorylation,<sup>(35)</sup> which in turn, stimulates Rac1 activation by the GEF.<sup>(36)</sup> Dock5 was shown to control epithelial cell spreading through its binding to CrkII.<sup>(37)</sup> The overall tyrosine phosphorylation profile in adherent OCs was not modified in the absence of Dock5 (Fig. 4F), but we found less p130Cas in phosphotyrosine-specific immunoprecipitates of *Dock5*<sup>-/-</sup> OC lysates (Fig. 4G, H). Consistently low levels of tyrosine phosphorylated p130Cas were found in *Dock5*<sup>-/-</sup> OC extracts immunoprecipitated with p130Cas-specific antibodies (Fig. 4I, J). We also observed increased CrkII phosphorylation (Fig. 4G, H), which is known to prevent binding of CrkII to p130Cas.<sup>(38)</sup> Conversely, phosphorylation of Pyk2, a partner of p130Cas in OCs involved in sealing zone formation,<sup>(39,40)</sup> remained unchanged in the absence of Dock5 (Fig. 4G, H). Taken together, these results suggest that the absence of Dock5 in OCs leads to adhesion defects associated with defective activation of Rac1 and p130Cas.

## A chemical inhibitor of Rac1 activation by Dock5 hinders OC bone-resorbing activity

To confirm the essential role of Rac1 activation by Dock5 in the resorption process, we sought for a chemical inhibitor of Dock5 exchange activity that is active in cell cultures. We

therefore took advantage of a yeast-based assay that we developed.<sup>(20,22)</sup> We constructed a yeast strain where Rac1 activation by Dock5 DHR2 induces the expression of the *His3* reporter gene (Fig. 5A), which leads to faster yeast growth in histidine-deprived medium (Fig. 5B). We screened a library of 2640 heterocyclic commercial chemical compounds, as described previously,<sup>(22)</sup> for molecules able to inhibit growth of Dock5 DHR2-expressing yeasts in histidine-deprived medium without affecting growth in histidine-complemented medium. Thus we identified C21: *N*-(3,5-dichlorophenyl)benzenesulfonamide (Fig. 5C). C21 efficiently inhibits the activation of Rac1 by Dock5 DHR2 in HEK293T cells (Fig. 5D) but has no effect on Rac1 activation by the GEF TrioN<sup>(22)</sup> (Fig. 5E). OC survival assays showed that C21 provokes OC death at concentrations above 25  $\mu$ M (Fig. 5F). Thus 25  $\mu$ M C21 efficiently inhibits the resorption of calcium phosphate matrices (not shown) and bone resorption, as assessed by measurement of CTX concentration in the culture medium of OCs (Fig. 5G). In parallel, control OCs grown in the presence of DMSO or 25  $\mu$ M C21 were stained for TRACP to ascertain that C21 was not toxic (not shown). A dose-response experiment confirmed that C21 efficiently inhibits bone resorption by OCs in vitro (Fig. 5H). These results show that a small chemical compound preventing Rac1 activation by Dock5 efficiently suppresses bone resorption by OCs in vitro.

### Dock5 deficiency leads to increased trabecular bone mass in the mouse

We explored the tissue distribution of Dock5 in mice. Interestingly, we found no activation of *Dock5* transcription in the bone-forming mature osteoblasts derived from MSCs (Fig. 6A), whereas the expression of osteoblast differentiation marker genes showed a very strong increase (Fig. 6B). Western blot analyses of protein extracts from a variety of mouse tissues showed that Dock5 is expressed predominantly in OCs, testis, and placenta (Fig. 6C). Although Dock5 is expressed in these latter tissues and in ovary (not shown), *Dock5*<sup>-/-</sup> mice breed normally (not shown), suggesting that Dock5 does not play an essential function in mouse reproduction. This shows that the expression of Dock5 is restricted to a very narrow set of tissues in mice, including bone-degrading OCs and excluding bone-forming osteoblasts.

Quantitative bone histomorphometry performed on histologic slices revealed that trabecular bone volume to total volume ratio (BV/TV) is increased over 30% in *Dock5*<sup>-/-</sup> mice compared with wild-type animals (19%  $\pm$  3.5% in *Dock5*<sup>-/-</sup> versus 14.3%  $\pm$  2.6% in *Dock5*<sup>+/+</sup>; Fig. 6D, E). In parallel, we found that OC number per bone surface (OC/mm) is identical in both genotypes (11.2  $\pm$  3.4 OC/mm in *Dock5*<sup>-/-</sup> versus 12.5  $\pm$  3.4 OC/mm in *Dock5*<sup>+/+</sup>; Fig. 6F, G). Together with our in vitro observations, these data are consistent with an essential role of Dock5 for bone resorption but not for differentiation of OCs.

### Discussion

Increased bone resorption by OCs is associated with various physiologic disorders and pathologic situations, including hormonal defects, inflammation, and cancer. Our study provides evidence that inhibition of Dock5 could be a novel approach to regulate bone loss. Our data highlight the essential role of this atypical Rac1 exchange factor in bone resorption; in the absence of Dock5, OCs differentiate but are unable to resorb bone owing to their



inability to form a sealing zone. We show that inhibition of Rac1 activation by Dock5 using a small chemical compound can modulate bone resorption. Finally, we found that *Dock5*<sup>-/-</sup> mice have increased trabecular bone mass associated with normal number of OCs, showing that Dock5 is also essential for bone resorption in vivo.

Targeting small GTPase signaling pathways using nitrogen-containing bisphosphonates (N-BPs) has long proven an efficient strategy to control bone resorption by OCs in a variety of pathologic situations.<sup>(41)</sup> N-BPs inhibit the C-terminal prenylation of small GTPases from the Ras, Rab, and Rho families, inducing the accumulation of unprenylated small GTPases and provoking OC dysfunction and death.<sup>(42)</sup> However, N-BPs target a wide range of small GTPases that control many signaling cascades, which may be a reason for the undesirable side effects arising from N-BPs-based treatments.<sup>(43,44)</sup> Considerable effort is currently being made to develop novel antiresorptive agents by targeting processes more specific to OCs, such as RANKL antibodies and cathepsin K inhibitors.<sup>(45)</sup> We found that Dock5 is expressed predominantly in OCs; in particular, it is not expressed in osteoblasts, the bone-forming cells. Furthermore, *Dock5*<sup>-/-</sup> mice do not present major phenotypic defects. This suggests that inhibiting Dock5 in vivo could reduce the activity of OCs without affecting bone formation and other physiologic functions. Therefore, targeting Dock5 exchange activity could represent a valuable strategy for the development of novel antiosteoporotic treatments.

We used several experimental approaches to investigate the function of Dock5 in OCs. While all consistently lead to the conclusion that Dock5 is essential for OC bone-resorbing activity, the experimental systems used showed minor discrepancies. In particular, we did not observe any toxic effect of *Dock5* shRNAs on differentiating BMMs into OCs, contrary to what we had observed in RAW264.7 cells.<sup>(16)</sup> This may reflect the high infection efficiency of RAW264.7 cells compared with BMMs because we never obtained complete silencing of Dock5 in primary cells. The toxic effect observed in RAW264.7 cells is most likely due to off-target effects resulting from high levels of shRNAs rather than complete silencing of Dock5 because differentiation of *Dock5*<sup>-/-</sup> BMMs into OCs does not result in cell death.

Rho GTPases are well-established regulators of the actin cytoskeleton, which is highly dynamic in OCs, in particular during the resorption process, when podosomes reorganize into a sealing zone.<sup>(4,7)</sup> We showed that among the many RhoGEF genes expressed in OCs, only *Dock5* and the RhoA GEF *Arhgef8* exhibit strong transcriptional activation during RANKL-induced osteoclastogenesis.<sup>(16)</sup> We confirm now that the expression of Dock5 protein is indeed much higher in OCs compared with BMMs. In line with our findings, Ha and colleagues reported a quantitative proteomic study<sup>(17)</sup> showing that after ATP6v0d2, which is critical for OC differentiation, Dock5 is the second most abundant membrane-associated protein differentially expressed in OCs as compared with macrophages. Our results did not reveal a role for Dock5 during OC differentiation per se. *Dock5*<sup>-/-</sup> mice have a normal number of OCs, and *Dock5*<sup>-/-</sup> BMMs efficiently differentiate in vitro into OCs that express all characteristic genes tested. Conversely, Rac1 was shown to be necessary for the expression of the OC markers TRACP and cathepsin K.<sup>(46)</sup> Therefore, it is likely that GEFs distinct from Dock5 are needed to activate Rac1 for the control of gene expression during

OC differentiation. In particular, the exchange factor Vav3 is required for Rac1 activation and expression of late OC differentiation markers *calcitonin receptor*, *TRACP*, and *cathepsin K*.<sup>(31)</sup>

Normal induction of the differentiation program suggests that the defects we observed in *Dock5*<sup>-/-</sup> OCs result from signaling defects, although we cannot exclude that important but as yet unidentified genes require Dock5 for their transcriptional activation during differentiation. We found that the steady-state activity of Rac1 is reduced in OCs lacking Dock5. Interestingly, we also found reduced phosphorylation of p130Cas in the absence of Dock5. In OCs, M-CSF was shown to induce the stable interaction of c-Fms with avβ3 integrin and p130Cas. This leads to the phosphorylation of p130Cas, which is involved in the formation of the sealing zone.<sup>(32-34)</sup> Moreover, Dock1 was shown to increase p130Cas phosphorylation and to positively regulate signaling from integrins to the p130Cas-Crk signaling complex,<sup>(35)</sup> which favors Rac1 activation.<sup>(47,48)</sup> Altogether, this information suggests that Dock5 and p130Cas could be involved in a common signaling network to control the activation of Rac1 in OCs. Vav3 is also required for the formation of the sealing zone.<sup>(31)</sup> Nevertheless, our findings suggest that the signaling pathways controlled by Dock5 and Vav3 during this process are distinct. Indeed, M-CSF and adhesion-stimulated activation of Rac1 requires Vav3,<sup>(31)</sup> whereas we found that it is independent of Dock5. M-CSF and adhesion were shown to activate Vav3, which is then recruited with Rac1 at the plasma membranes of OCs.<sup>(49)</sup> We found that Dock5 associates with the OC podosome belt. A possible hypothesis would be that Dock5 and Vav3 regulate Rac1 activation at distinct locations in OCs and at different phases of the bone-resorption cycle (Fig. 7). For efficient resorption, OCs alternate between spreading and resorption steps that involve disassembly and re-formation of the sealing zone.<sup>(7)</sup> After the end of a resorption step, activation of c-Fms by M-CSF and of integrins through adhesion would recruit and activate Vav3 at the plasma membrane, leading to rapid activation of Rac1.<sup>(28,49)</sup> This would allow the OC spreading and actin remodeling necessary for the initiation of new sealing zone formation (Fig. 7B). Then stable interaction of c-Fms with avβ3 by promoting the assembly of a signaling scaffold involving the p130Cas-CrkII complex<sup>(34)</sup> would sustain robust activation of Rac1 by Dock5 at the actin ring. This would allow the stabilization of the sealing zone necessary for efficient bone resorption (Fig. 7C).

*Dock5*<sup>-/-</sup> mice have increased trabecular bone volume with normal number of OCs. This is in line with our in vitro observations showing that Dock5 is essential for resorption but not for OC differentiation. Although the effect of Dock5 suppression is very drastic for OC activity in vitro, *Dock5*<sup>-/-</sup> animals do not show a severe bone mass increase. The phenotype of *Dock5*<sup>-/-</sup> mice is consistent with the moderate osteopetrotic phenotype reported for mice with targeted deletion of Rac1 in OCs.<sup>(46)</sup> The moderate phenotype of *Dock5*<sup>-/-</sup> mice may be due to adaptive physiologic mechanisms that may compensate for the low resorbing activity of OCs in vivo but are not activated in the in vitro model of cultured OCs. In particular, we did not observe increased expression of *Vav3*, *Dock1*, or *Dock2* in *Dock5*<sup>-/-</sup> OCs in culture. These or other Rac1 GEFs expressed in OCs<sup>(16)</sup> may complement in part Dock5 deficiency in vivo. In line with this hypothesis, we reported previously that Dock1 and Dock5 are partially redundant during muscle fiber formation.<sup>(14)</sup> Consistent with the restricted distribution of Dock5, *Dock5*<sup>-/-</sup> mice do not present major phenotypic defects. In

particular, they are fertile and breed normally, whereas Dock5 is expressed in testis and placenta, suggesting that Dock5 may not play an essential role in these tissues. Therefore, inhibiting Dock5 to limit bone resorption is expected to have limited side effects on other physiologic functions.

Using *N*-(3,5-dichlorophenyl)benzenesulfonamide (C21), we show that the inhibition of Dock5 exchange activity toward Rac1 can efficiently reduce OC bone-resorbing activity. This confirms that the activation of Rac1 by Dock5 plays a major role in the resorption process. Furthermore, the identification of this model chemical compound suggests that Dock5 activity can be reduced using small-cell permeant molecules and that developing inhibitors of Rac1 activation by Dock5 represents a novel approach to control bone resorption. C21 is not a general inhibitor of Rac activation because it does not affect Trio exchange activity. Nevertheless, we found that C21 also affects Dock1 and to a lesser extent Dock2 exchange activities (our unpublished observations). Although the efficiency seems lower on those two GEFs compared with Dock5, this was expected given the high level of similarity between the three DHR2 domains. Therefore, the toxic effect we observed on OCs when increasing the concentration of C21 may result from the inhibition of Dock1 and Dock2 or other exchange factors essential for the survival of OCs. We identified C21 using a screening methodology in yeast that we previously validated for the exchange factor Trio.<sup>(20,22)</sup> It could be valuable to screen more chemical compound libraries with such an assay to provide a novel source of chemical frameworks from which to develop original antiresorptive molecules.

In summary, we have shown that Dock5 is essential for formation of the sealing zone and then for bone resorption by OCs in vitro and in vivo. Moreover, we show that inhibition of Rac1 activation by Dock5 using a small chemical compound can efficiently reduce bone resorption by OCs. The expression of Dock5 is restricted mainly to OCs, and it is absent from osteoblasts. Therefore, developing Dock5 inhibitors appears to be a novel approach to generating original antiresorptive molecules that would target OC activity with reduced side effects.

## Supplementary Material

Refer to Web version on PubMed Central for supplementary material.

## Acknowledgments

We want to thank Romain Dacquin for technical advice in performing the bone histology and Jean-Paul Leonetti for sharing his chemical compound library. This work was supported by grants from the Fondation pour la Recherche Médicale (Grant DVO20081013473 to AB), from the Ligue contre le Cancer (Grant 7FI9556JQSC, comité de l'Aude, to AB), from the Arthritis Foundation Courtins (Grant OTP30713 to AB), and the Canadian Institute of Health Research (CIHR to J-FC). VV was a recipient of a postdoctoral fellowship from the Association pour la Recherche sur le Cancer. J-FC holds a CIHR New Investigator award.

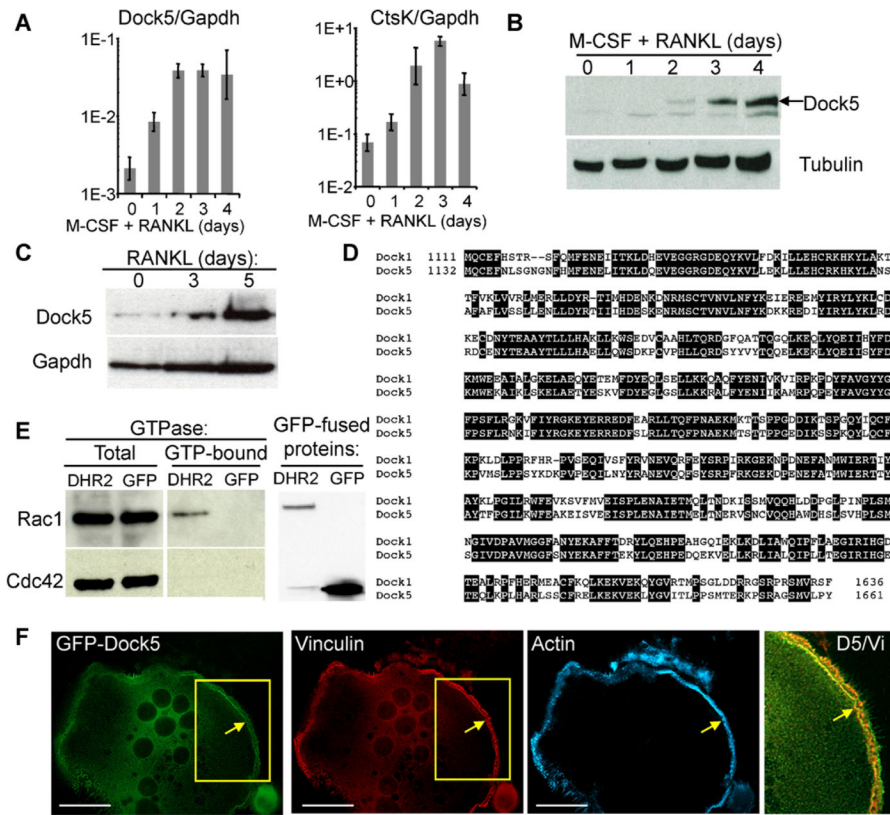
## References

1. Weitzmann MN, Pacifici R. Estrogen deficiency and bone loss: an inflammatory tale. *J Clin Invest.* 2006; 116:1186–1194. [PubMed: 16670759]

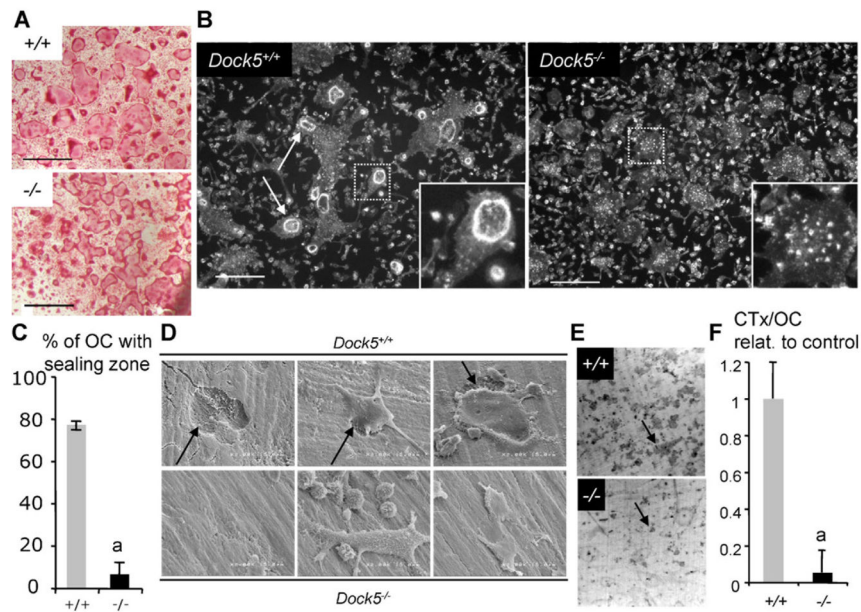
2. Teitelbaum SL, Ross FP. Genetic regulation of osteoclast development and function. *Nat Rev Genet.* 2003; 4:638–649. [PubMed: 12897775]
3. Jurdic P, Saltel F, Chabadel A, Destaing O. Podosome and sealing zone: specificity of the osteoclast model. *Eur J Cell Biol.* 2006; 85:195–202. [PubMed: 16546562]
4. Luxenburg C, Geblinger D, Klein E, et al. The architecture of the adhesive apparatus of cultured osteoclasts: from podosome formation to sealing zone assembly. *PLoS ONE.* 2007; 2:e179. [PubMed: 17264882]
5. Vaananen HK, Laitala-Leinonen T. Osteoclast lineage and function. *Arch Biochem Biophys.* 2008; 473:132–138. [PubMed: 18424258]
6. Kim K, Lee SH, Ha Kim J, Choi Y, Kim N. NFATc1 induces osteoclast fusion via up-regulation of Atp6v0d2 and the dendritic cell-specific transmembrane protein (DC-STAMP). *Mol Endocrinol.* 2008; 22:176–185. [PubMed: 17885208]
7. Saltel F, Destaing O, Bard F, Eichert D, Jurdic P. Apatite-mediated actin dynamics in resorbing osteoclasts. *Mol Biol Cell.* 2004; 15:5231–5241. [PubMed: 15371537]
8. Nakamura I, Duong le T, Rodan SB, Rodan GA. Involvement of alpha(v)beta3 integrins in osteoclast function. *J Bone Miner Metab.* 2007; 25:337–344. [PubMed: 17968485]
9. Ory S, Brazier H, Pawlak G, Blangy A. Rho GTPases in osteoclasts: orchestrators of podosome arrangement. *Eur J Cell Biol.* 2008; 87:469–477. [PubMed: 18436334]
10. Rossman KL, Der CJ, Sondek J. GEF means go: turning on RHO GTPases with guanine nucleotide-exchange factors. *Nat Rev Mol Cell Biol.* 2005; 6:167–180. [PubMed: 15688002]
11. Cote JF, Vuori K. Identification of an evolutionarily conserved superfamily of DOCK180-related proteins with guanine nucleotide exchange activity. *J Cell Sci.* 2002; 115(Pt 24):4901–4913. [PubMed: 12432077]
12. Meller N, Merlot S, Guda C. CZH proteins: a new family of Rho-GEFs. *J Cell Sci.* 2005; 118(Pt 21):4937–4946. [PubMed: 16254241]
13. Cote JF, Vuori K. GEF what? Dock180 and related proteins help Rac to polarize cells in new ways. *Trends Cell Biol.* 2007; 17:383–393. [PubMed: 17765544]
14. Laurin M, Fradet N, Blangy A, Hall A, Vuori K, Cote JF. The atypical Rac activator Dock180 (Dock1) regulates myoblast fusion in vivo. *Proc Natl Acad Sci U S A.* 2008; 105:15446–15451. [PubMed: 18820033]
15. Pajcini KV, Pomerantz JH, Alkan O, Doyonnas R, Blau HM. Myoblasts and macrophages share molecular components that contribute to cell-cell fusion. *J Cell Biol.* 2008; 180:1005–1019. [PubMed: 18332221]
16. Brazier H, Stephens S, Ory S, Fort P, Morrison N, Blangy A. Expression profile of RhoGTPases and RhoGEFs during RANKL-stimulated osteoclastogenesis: identification of essential genes in osteoclasts. *J Bone Miner Res.* 2006; 21:1387–1398. [PubMed: 16939397]
17. Ha BG, Hong JM, Park JY, et al. Proteomic profile of osteoclast membrane proteins: identification of Na<sup>+</sup>/H<sup>+</sup> exchanger domain containing 2 and its role in osteoclast fusion. *Proteomics.* 2008; 8:2625–2639. [PubMed: 18600791]
18. Fritz V, Noel D, Bouquet C, et al. Antitumoral activity and osteogenic potential of mesenchymal stem cells expressing the urokinase-type plasminogen antagonist amino-terminal fragment in a murine model of osteolytic tumor. *Stem Cells.* 2008; 26:2981–2990. [PubMed: 18757301]
19. Brazier H, Pawlak G, Vives V, Blangy A. The Rho GTPase Wrch1 regulates osteoclast precursor adhesion and migration. *Int J Biochem Cell Biol.* 2009; 41:1391–1401. [PubMed: 19135548]
20. Blangy A, Bouquier N, Gauthier-Rouviere C, et al. Identification of TRIO-GEFD1 chemical inhibitors using the yeast exchange assay. *Biol Cell.* 2006; 98:511–522. [PubMed: 16686599]
21. De Toledo M, Colombo K, Nagase T, Ohara O, Fort P, Blangy A. The yeast exchange assay, a new complementary method to screen for Dbl-like protein specificity: identification of a novel RhoA exchange factor. *FEBS Lett.* 2000; 480:287–292. [PubMed: 11034346]
22. Bouquier N, Vignal E, Charrasse S, et al. A cell active chemical GEF inhibitor selectively targets the Trio/RhoG/Rac1 signaling pathway. *Chem Biol.* 2009; 16:657–666. [PubMed: 19549603]
23. Kitamura T, Koshino Y, Shibata F, et al. Retrovirus-mediated gene transfer and expression cloning: powerful tools in functional genomics. *Exp Hematol.* 2003; 31:1007–1014. [PubMed: 14585362]

24. Choi SJ, Han JH, Roodman GD. ADA M8: a novel osteoclast stimulating factor. *J Bone Miner Res.* 2001; 16:814–822. [PubMed: 11341326]
25. Andre E, Bastide L, Villain-Guillot P, Latouche J, Rouby J, Leonetti JP. A multiwell assay to isolate compounds inhibiting the assembly of the prokaryotic RNA polymerase. *Assay Drug Dev Technol.* 2004; 2:629–635. [PubMed: 15674021]
26. Cote JF, Vuori K. In vitro guanine nucleotide exchange activity of DHR-2/DOCKER/CZH2 domains. *Methods Enzymol.* 2006; 406:41–57. [PubMed: 16472648]
27. Yang J, Zhang Z, Roe SM, Marshall CJ, Barford D. Activation of Rho GTPases by DOCK exchange factors is mediated by a nucleotide sensor. *Science.* 2009; 325:1398–1402. [PubMed: 19745154]
28. Faccio R, Takeshita S, Colaianni G, et al. M-CSF regulates the cytoskeleton via recruitment of a multimeric signaling complex to c-Fms Tyr-559/697/721. *J Biol Chem.* 2007; 282:18991–18999. [PubMed: 17420256]
29. Faccio R, Novack DV, Zallone A, Ross FP, Teitelbaum SL. Dynamic changes in the osteoclast cytoskeleton in response to growth factors and cell attachment are controlled by beta3 integrin. *J Cell Biol.* 2003; 162:499–509. [PubMed: 12900398]
30. Yan J, Chen S, Zhang Y, et al. Rac1 mediates the osteoclast gains-in-function induced by haploinsufficiency of Nf1. *Hum Mol Genet.* 2008; 17:936–948. [PubMed: 18089636]
31. Faccio R, Teitelbaum SL, Fujikawa K, et al. Vav3 regulates osteoclast function and bone mass. *Nat Med.* 2005; 11:284–290. [PubMed: 15711558]
32. Elsegood CL, Zhuo Y, Wesolowski GA, Hamilton JA, Rodan GA, Duong le T. M-CSF induces the stable interaction of cFms with alphaVbeta3 integrin in osteoclasts. *Int J Biochem Cell Biol.* 2006; 38:1518–1529. [PubMed: 16600665]
33. Nakamura I, Jimi E, Duong LT, et al. Tyrosine phosphorylation of p130Cas is involved in actin organization in osteoclasts. *J Biol Chem.* 1998; 273:11144–11149. [PubMed: 9556601]
34. Nakamura I, Rodan GA, Duong le T. Distinct roles of p130Cas and c-Cbl in adhesion-induced or macrophage colony-stimulating factor-mediated signaling pathways in perfusion osteoclasts. *Endocrinology.* 2003; 144:4739–4741. [PubMed: 12959979]
35. Kiyokawa E, Hashimoto Y, Kurata T, Sugimura H, Matsuda M. Evidence that DOCK180 up-regulates signals from the CrkII-p130(Cas) complex. *J Biol Chem.* 1998; 273:24479–24484. [PubMed: 9733740]
36. Kiyokawa E, Hashimoto Y, Kobayashi S, Sugimura H, Kurata T, Matsuda M. Activation of Rac1 by a Crk SH3-binding protein, DOCK180. *Genes Dev.* 1998; 12:3331–3336. [PubMed: 9808620]
37. Sanders MA, Ampasala D, Basson MD. DOCK5 and DOCK1 regulate Caco-2 intestinal epithelial cell spreading and migration on collagen IV. *J Biol Chem.* 2009; 284:27–35. [PubMed: 19004829]
38. Kobashigawa Y, Sakai M, Naito M, et al. Structural basis for the transforming activity of human cancer-related signaling adaptor protein CRK. *Nat Struct Mol Biol.* 2007; 14:503–510. [PubMed: 17515907]
39. Gil-Henn H, Destaing O, Sims NA, et al. Defective microtubule-dependent podosome organization in osteoclasts leads to increased bone density in Pyk2(−/−) mice. *J Cell Biol.* 2007; 178:1053–1064. [PubMed: 17846174]
40. Lakkakorpi PT, Nakamura I, Nagy RM, Parsons JT, Rodan GA, Duong LT. Stable association of PYK2 and p130(Cas) in osteoclasts and their co-localization in the sealing zone. *J Biol Chem.* 1999; 274:4900–4907. [PubMed: 9988732]
41. Rodan GA, Martin TJ. Therapeutic approaches to bone diseases. *Science.* 2000; 289:1508–1514. [PubMed: 10968781]
42. Russell RG, Watts NB, Ebetino FH, Rogers MJ. Mechanisms of action of bisphosphonates: similarities and differences and their potential influence on clinical efficacy. *Osteoporos Int.* 2008; 19:733–759. [PubMed: 18214569]
43. Kennel KA, Drake MT. Adverse effects of bisphosphonates: implications for osteoporosis management. *Mayo Clin Proc.* 2009; 84:632–637. quiz 638. [PubMed: 19567717]
44. Recker RR, Lewiecki EM, Miller PD, Reiffel J. Safety of bisphosphonates in the treatment of osteoporosis. *Am J Med.* 2009; 122(2 Suppl):S22–32.

45. Deal C. Future therapeutic targets in osteoporosis. *Curr Opin Rheumatol.* 2009; 21:380–385. [PubMed: 19461517]
46. Wang Y, Lebowitz D, Sun C, Thang H, Grynblas MD, Glogauer M. Identifying the relative contributions of rac1 and rac2 to osteoclastogenesis. *J Bone Miner Res.* 2008; 23:260–270. [PubMed: 17922611]
47. Sharma A, Mayer BJ. Phosphorylation of p130Cas initiates Rac activation and membrane ruffling. *BMC Cell Biol.* 2008; 9:50. [PubMed: 18793427]
48. Smith HW, Marra P, Marshall CJ. uPAR promotes formation of the p130Cas-Crk complex to activate Rac through DOCK180. *J Cell Biol.* 2008; 182:777–790. [PubMed: 18725541]
49. Sakai H, Chen Y, Itokawa T, Yu KP, Zhu ML, Insogna K. Activated c-Fms recruits Vav and Rac during CSF-1-induced cytoskeletal remodeling and spreading in osteoclasts. *Bone.* 2006; 39:1290–1301. [PubMed: 16950670]

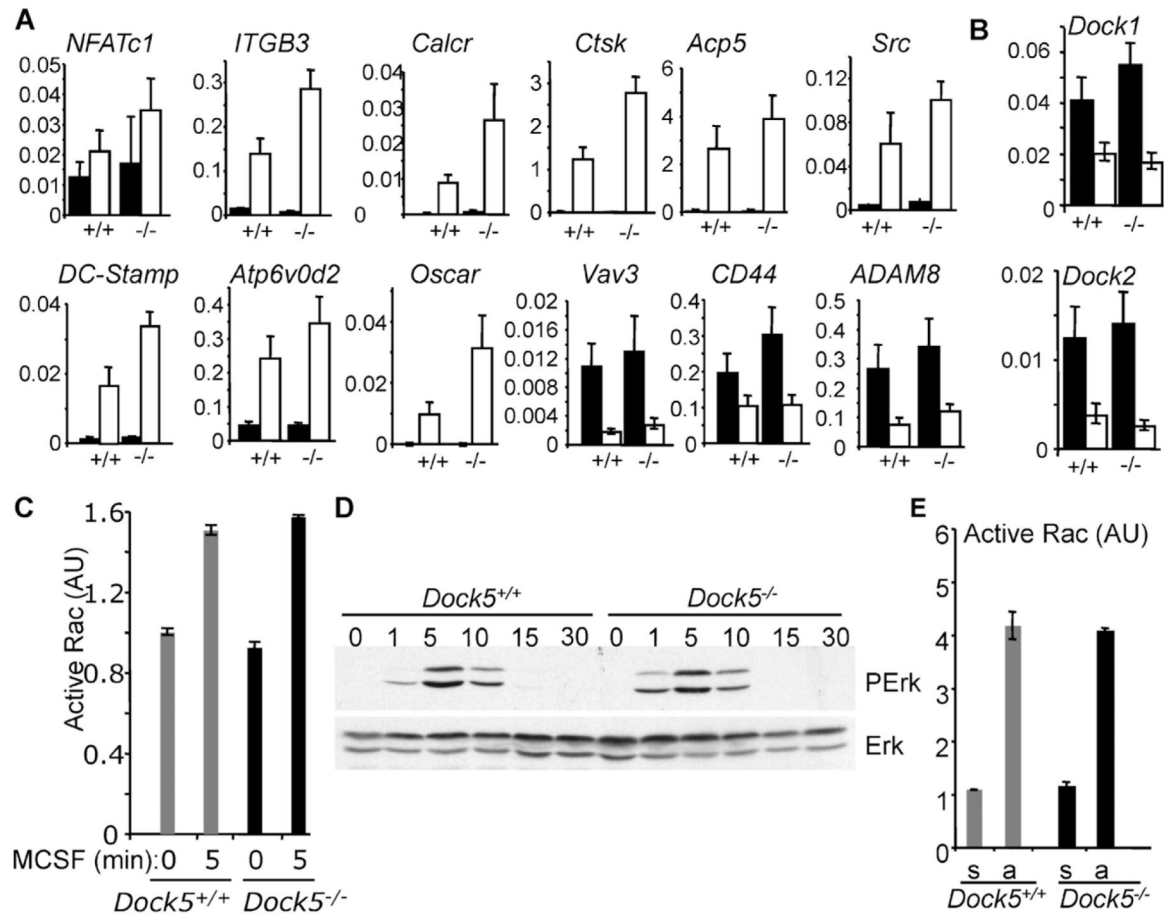


**Fig. 1.** Dock5 is a Rac1 exchange factor expressed in OCs. (A) Total RNA of BMMs induced for differentiation in the presence of RANKL and M-CSF was extracted on days 0, 1, 2, 3, and 4, and levels of *Dock5* and *cathepsin K (CtsK)* mRNA relative to *Gapdh* mRNA were determined by RT-PCR. (B, C) Total cell extracts were prepared from panel B BMMs treated as in panel A or panel C from RAW264.7 cells grown for the indicated time in the presence of RANKL. Dock5 protein expression was visualized by Western blot. (D) Alignment of the amino acid sequences of the DHR2 exchange domains of mouse Dock5 and Dock1.<sup>(11)</sup> Black background highlights residues conserved between the two sequences. (E) Total cell extracts were prepared from 293T cells expressing GFP-fused Dock5-DHR2 or GFP and submitted to GTP-trapping using the GST-fused CRIB domain of PAK1. Pulled-down and total Rac1 and Cdc42 (left panel) and GFP fusion proteins in total cell extracts (right panel) were revealed by Western blot. (F) Localization of GFP-tagged full-length Dock5 (green) expressed in RAW264.7-derived OCs was visualized by fluorescence microscopy after staining for vinculin (red) and F-actin (blue) to reveal the podosome belt. Last panel is an enlarged view of boxed areas where yellow color reveals colocalization of Dock5 and vinculin. Scale bar = 20  $\mu$ m.

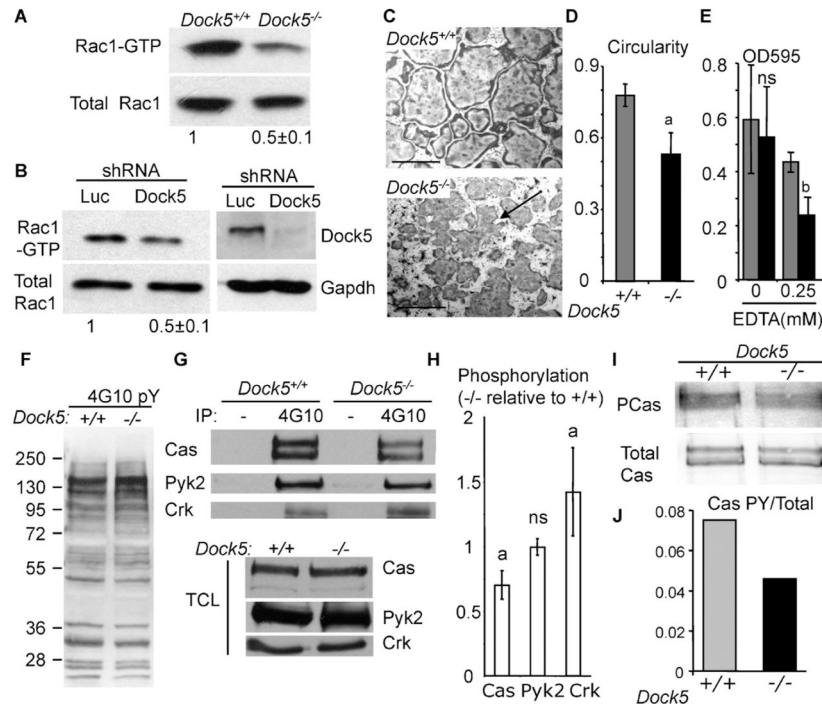
**Fig. 2.**

*Dock5* is necessary for bone resorption by OCs derived from BMMs. (A) OCs were differentiated from *Dock5*<sup>+/+</sup> (+/+) and *Dock5*<sup>-/-</sup> (-/-) BMMs and stained for TRACP activity. Scale bars = 200  $\mu$ m. (B) OCs were differentiated on Osteologic Biocoat from *Dock5*<sup>+/+</sup> and *Dock5*<sup>-/-</sup> BMMs and stained for actin to reveal the sealing zones (*arrows*). Insets show enlarged boxed areas. Scale bars = 100  $\mu$ m. (C) Proportion of OCs obtained as in panel B with a sealing zone. Graph shows average and SD of three independent OC preparations counting over 300 cells. <sup>a</sup>*p* < .001, Mann-Whitney test. (D) Scanning electron micrographs showing OCs differentiated on bone slices. Arrows point at resorption pits. (E) Bone slices from panel D were stained with WGA lectin to reveal resorption pits (*arrows*). (F) CTX concentrations measured in the culture medium of OCs grown on bone slices as in panels D and E. Graph shows average and SD CTX concentration per OC relative to *Dock5*<sup>+/+</sup> control OC from three independent experiments performed in triplicate. <sup>a</sup>*p* < .001 Mann-Whitney test.

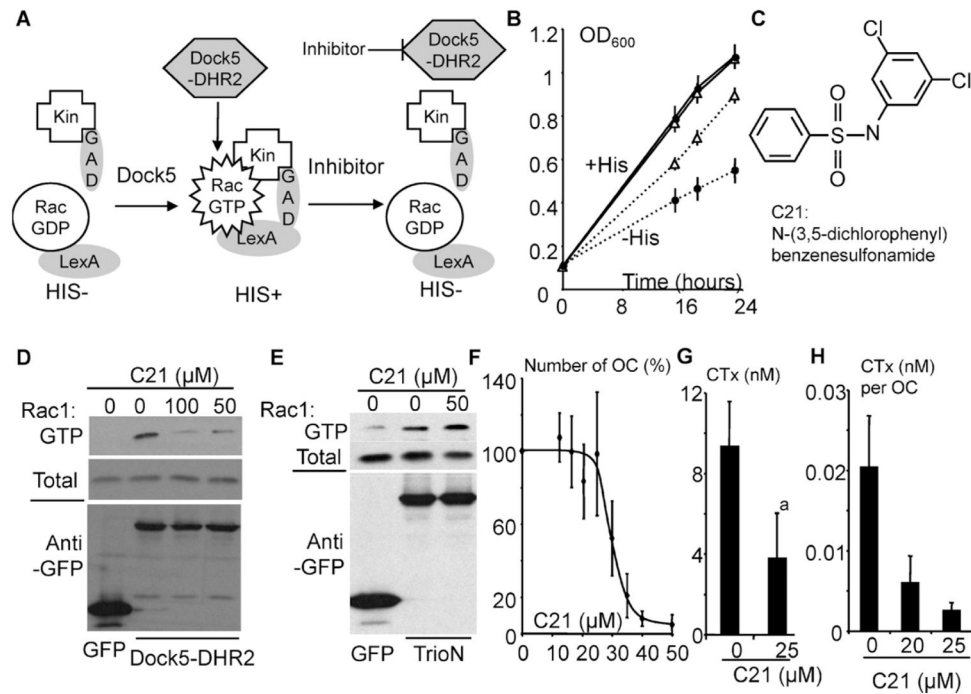


**Fig. 3.**

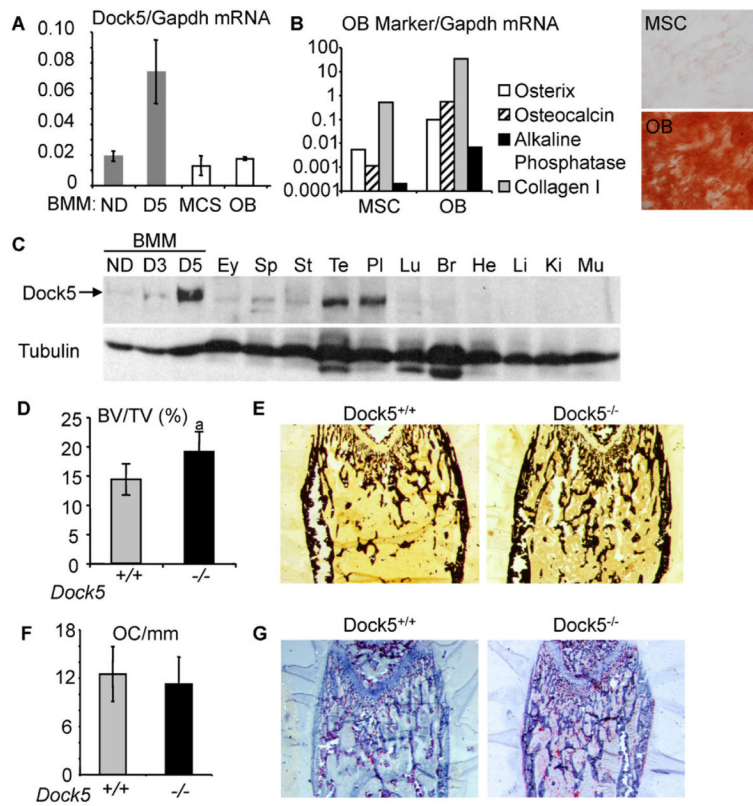
Dock5 is dispensable for the expression of OC characteristic genes and for Rac1 activation in response to M-CSF and adhesion. (A, B) Total RNAs were prepared from *Dock5*<sup>+/+</sup> (+/+) and *Dock5*<sup>-/-</sup> (-/-) BMMs grown for 5 days in the presence of M-CSF (black bars) or RANKL and M-CSF (white bars). mRNAs levels of OC characteristic genes (A) and from *Dock1* and *Dock2* (B) relative to *Gapdh* were determined by RT-PCR. (C) Rac1 activity was measured by G-LISA in *Dock5*<sup>+/+</sup> and *Dock5*<sup>-/-</sup> OCs on day 4 of differentiation stimulated with 100 ng/mL of M-CSF for the indicated amount of time. (D) The levels of total and phosphorylated Erk1/2 were determined by Western blot in *Dock5*<sup>+/+</sup> and *Dock5*<sup>-/-</sup> OCs stimulated with M-CSF as in panel C. (E) Rac1 activity was measured by G-LISA in *Dock5*<sup>+/+</sup> and *Dock5*<sup>-/-</sup> OCs on day 4 of differentiation lifted and left in suspension (s) or replated onto vitronectin-coated plates for 30 minutes (a). Panels C and E show average active Rac1 and SD of duplicate measures in one experiment representative of two independent OC preparations.



**Fig. 4.** Dock5-deficient OCs have less active Rac1 and adhesion defects and reduced p130Cas phosphorylation. (A) Western blot showing total and GTP-bound Rac1 in extracts of *Dock5*<sup>-/-</sup> and *Dock5*<sup>+/+</sup> OCs. (B) Western blots showing total and GTP-bound Rac1 (*left panel*) and Dock5 and Gapdh (*right panel*) in extracts of RAW264.7-derived OCs expressing Dock5 (shDock5) or control (shLuc) shRNAs. Panels A and B show average and SD active Rac1 levels in Dock5-deficient OCs relative to controls in two independent experiments; Western blots show one experiment. (C) *Dock5*<sup>+/+</sup> and *Dock5*<sup>-/-</sup> OCs were stained for TRACP activity to reveal global cell shape. Scale bars = 200  $\mu$ m. (D) OC average and SD circularity from four independent OC preparations measuring at least 60 OCs from four independent microscope fields in each experiment. <sup>a</sup> $p < .001$ , Mann-Whitney test. (E) OCs remaining bound after 5 minutes of incubation with the indicated concentration of EDTA, determined by crystal violet staining. Graph represents average and SD of two independent experiments performed in triplicates. <sup>b</sup> $p < .01$ , n.s. = non significant change, Mann-Whitney test. (F) Western blot revealing global tyrosine phosphorylation with 4G10 antibody in OC lysates. (G) Western blots showing p130Cas (Cas), Pyk2, and Crk in control (-) or 4G10 immunoprecipitates (IP) and in total lysates (TCL). (H) Average and SD levels of p130Cas (Cas), Pyk2, and Crk phosphorylation in OCs from two independent experiments, one is shown in panel G. <sup>a</sup> $p < .001$ , n.s. = nonsignificant change, Mann-Whitney test. (I) Western blot showing phosphorylated p130Cas (PCas) revealed by 4G10 and total p130Cas (Cas) in p130Cas immunoprecipitates of OC lysates. (J) Quantification of phosphorylated versus total p130Cas in the experiment shown in panel I.

**Fig. 5.**

Inhibition of bone resorption by an inhibitor of Rac1 activation by Dock5. (A) Principle of the yeast exchange assay used to identify inhibitors of Dock5 exchange activity. Wild-type Rac1 is fused to LexA DNA-binding domain (LexA) and its effector kinectin (Kin) to the GAL4 activation domain (GAD). Expression of Dock5-DHR2 activates Rac1, which binds to kinectin, leading to expression of His3 and then yeast auxotrophy for histidine. Inhibitors of Dock5-DHR2 revert Rac1 activation. (B) Growth curves of yeasts expressing Rac1 and kinectin with (*open triangles*) and without (*dots*) Dock5-DHR2 in medium complemented (*plain lines*) or not (*dotted lines*) with histidine. (C) Structure of *N*-(3,5-dichlorophenyl)benzenesulfonamide (C21). (D) Western blots showing total and GTP-bound Rac1 (*upper panels*) and GFP and GFP-fused Dock5-DHR2 in extracts of 293T cells treated for 1 hour with the indicated concentrations of C21 in the presence of 1% DMSO. (E) Western blots showing total and GTP-bound Rac1 (*upper panels*) and GFP and GFP-fused TrioN in extracts of 293T cells treated as in panel D. (F) Number of OCs (OC) after a 24-hour incubation with the indicated concentrations of C21, expressed as a percent of DMSO control (0 μM C21). Graph shows average and SD of two to three independent experiments performed in triplicate. (G) CTX concentration in the medium of OCs on bone in the absence (0) or presence of 25 μM C21. Graph shows average and SD of three experiments performed in duplicate with independent OC preparations. <sup>a</sup>*p* < .001, Mann-Whitney test. (H) CTX production per OC in the presence of the indicated concentration of C21. Graph shows average and SD CTX concentration per OC in one experiment performed in triplicate.

**Fig. 6.**

Suppression of *Dock5* leads to reduced trabecular bone mass in mice. (A) Levels of *Dock5* mRNA relative to *Gapdh* mRNA determined by RT-PCR in BMMs grown with M-CSF (ND) or differentiated into OCs for 5 days (D5) and in proliferating MSCs and MSC-derived osteoblasts (OB). (B) mRNA levels of the indicated osteoblast differentiation marker genes relative to *Gapdh* in proliferating MSCs and osteoblasts from panel A and mineralization activity of the osteoblasts revealed by alizarin red S staining. (C) Total proteins extracted from BMMs grown with M-CSF (ND) or for 3 and 5 days with M-CSF and RANKL and from various mouse tissues (Ey = eye; Sp = spleen; St = stomach; Te = testis; Pl = placenta; Lu = lung; Br = brain; He = heart; Li = liver; Ki = kidney; Mu = muscle) were analyzed by Western blot with antibodies against *Dock5* and tubulin for normalization. (D) Percent bone volume/total volume (BV/TV) in distal femurs of 7-week-old mice ( $n = 6$ ). <sup>a</sup> $p < .001$ , Mann-Whitney test. (E) Histologic section showing distal femur of 7-week-old mouse stained with von Kossa to reveal mineralized tissue. (F) OC number per bone perimeter (OC/mm) in distal femurs of 7-week-old mice ( $n = 6$ ). (G) Histologic sections from distal femurs of 7-week-old mice stained for TRACP activity to visualize OCs and counterstained with hematoxylin to visualize bone trabeculae.

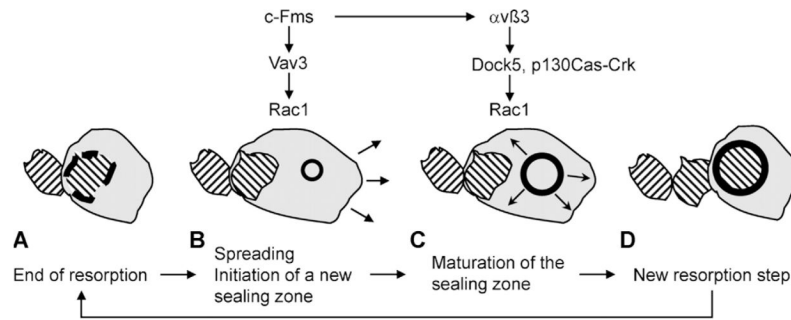


**Fig. 7.**

Model for the respective functions of Dock5 and Vav3 during OC resorption cycle. OCs alternate between resorption and spreading phases.<sup>(7)</sup> (A) At the end of a resorption phase, the sealing zone disassembles (*thick black dotted line*) around the newly formed resorption pit (*dashed area*). (B) Under the stimulation of M-CSF, Vav3 gets activated and, in turn, activates Rac1 downstream of c-Fms, allowing the OC to spread away from its previous resorption pits (*arrows*), initiating a new sealing zone (*thick black circle*). (C) Then the stable interaction of c-Fms with  $\alpha v \beta 3$  promotes assembly of the p130Cas-CrkII signaling scaffold to sustain robust activation of Rac1 by Dock5, allowing enlargement and stabilization of the sealing zone (*arrows*) for an efficient new bone-resorption step (D).